

Nitric oxide reactivity of Cu(II) complexes of tetra- and pentadentate ligands: structural influence in deciding the reduction pathway

Cite this: *Dalton Trans.*, 2013, **42**, 5731

Pankaj Kumar, Apurba Kalita and Biplab Mondal*

Four Cu(II) complexes, **1**, **2**, **3** and **4**, are synthesized with ligands, **L**₁, **L**₂, **L**₃ and **L**₄ [**L**₁ = *N*1,*N*2-bis((pyridin-2-yl)methyl)ethane-1,2-diamine; **L**₂ = *N*1,*N*3-bis((pyridin-2-yl)methyl)propane-1,3-diamine; **L**₃ = *N*1,*N*1,*N*2-tris((pyridin-2-yl)methyl)ethane-1,2-diamine; **L**₄ = *N*1-((1-methyl-1*H*-imidazol-2-yl)methyl)-*N*1,*N*2-bis((pyridin-2-yl)methyl)ethane-1,2-diamine], respectively, as their perchlorate salts. The complexes were characterized by various spectroscopic techniques as well as single crystal X-ray structure determination. Nitric oxide reactivities of the complexes were studied in acetonitrile as well as methanol solvent. It has been found that the ligand frameworks have a considerable effect in controlling the mechanism of the reduction of a Cu(II) center by nitric oxide. The flexibility of the ligand/s for a Cu(II) complex to attain a trigonal bipyramidal geometry after NO coordination is found to be the most important parameter in dictating the pathway for their interaction. In the present study, all the four compounds, because of structural constraints, were found to follow a deprotonation pathway for the reduction of a Cu(II) center by nitric oxide rather than [Cu^{II}-NO] intermediate formation. All the ligands were found to yield an *N*-nitrosoamine product along with the reduction of Cu(II) centers by nitric oxide.

Received 11th September 2012,
Accepted 4th September 2013

DOI: 10.1039/c3dt32580f

www.rsc.org/dalton

Introduction

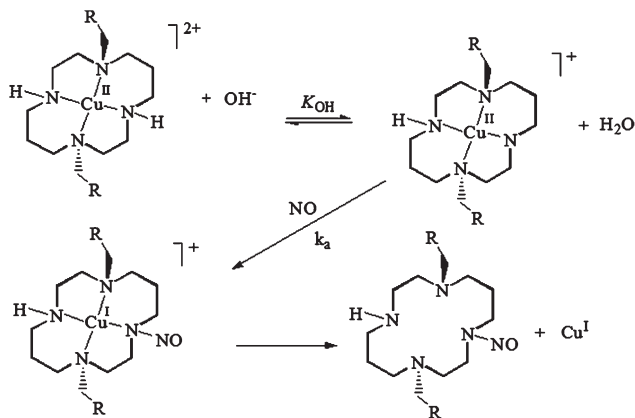
Activation of nitric oxide through its coordination to transition metal ions has been a subject of interest for chemists and biochemists since its discovery as it is found to play various roles in mammalian biology.^{1–6} In ferriheme proteins, nitric oxide is known to coordinate to form an iron(III)-nitrosyl intermediate prior to the pH dependent reduction of the Fe(III) center.^{4,5} In subsequent steps, the hydroxide ion attacks the activated nitrosonium group to afford a nitrite ion.⁴ The ferrous protein thus formed reacts with the excess of nitric oxide to form stable ferroheme nitrosyl.^{6–8} In copper-proteins, for instance, cytochrome *c* oxidase and laccase, the reduction of Cu(II) to Cu(I) by nitric oxide has been known for a long time.^{9–12} Wayland and others suggested a mechanism closer to that of ferriheme reduction involving the initial nitric oxide coordination to the Cu(II) center to form [Cu^{II}-NO ↔ Cu^I-NO⁺].¹³ Recently, a

number of examples of the interaction of nitric oxide with copper(II) complexes leading to the reduction of the Cu(II) center have been reported in the literature. Nitric oxide is shown to reduce the Cu(II) center in [Cu(dmp)₂(X)]²⁺ (dmp = 2,9-dimethyl-1,10-phenanthroline, X = solvent) and analogous complexes through an inner-sphere pathway.^{14,15} In different examples, the Cu(II) center of [Cu^{II}(DAC)]²⁺ and [Cu(mtd)]²⁺ {DAC = 1,8-bis(9-anthracylmethyl) derivative of the macrocyclic tetraamine cyclam (1,4,8,11-tetraazacyclotetradecane) and mtd = 5,5,7,12,12,14-hexamethyl-1,4,8,11-tetraazacyclotetradecane} in methanol is reported to be reduced by nitric oxide with concomitant nitrosation of the ligands.¹⁶ Quantitative and theoretical studies suggested that the reaction in these cases proceeds through a pathway analogous to the inner-sphere mechanism for electron transfer between two metal centers through a bridging ligand where NO is the reductant, Cu(II) the oxidant and the coordinated amido anion behaves as the bridging ligand (Scheme 1).

Demetallation of the macrocyclic ring after the reduction of Cu(II) takes place owing to the preference of Cu(I) for tetrahedral coordination and the decreased donor ability of the nitrosated ligand. The formation of Ru(II)-dinitrogen complex, [Ru(NH₃)₅(N₂)]²⁺, from the reaction of [Ru(NH₃)₆]³⁺ with NO in alkaline solution was proposed to follow a similar mechanistic pathway.¹⁷ Nitrosation of a coordinated amide ligand with the

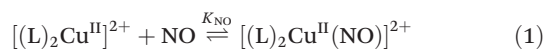
Department of Chemistry, Indian Institute of Technology Guwahati, Assam 781039, India. E-mail: biplab@iitg.ernet.in

† Electronic supplementary information (ESI) available: All the characterization data for the ligands and the complexes; UV-visible, EPR spectra of all the complexes before and reaction with nitric oxide are included. CCDC 910909–910912. For ESI and crystallographic data in CIF or other electronic format see DOI: 10.1039/c3dt32580f



simultaneous reduction of Ru(III) to Ru(II) results in a coordinated nitroso amine, which on subsequent dehydration affords the coordinated dinitrogen complex.

On the other hand, a series of Cu(II) complexes of N-donor ligands have been reported to form unstable $[\text{Cu}^{\text{II}}\text{-NO}]$ intermediates on reaction with nitric oxide prior to the reduction of Cu(II). For example, in Cu(II) complexes of tripodal tetradentate ligands, $[\text{Cu}^{\text{II}}(\text{tren})(\text{CH}_3\text{CN})]^{2+}$, $[\text{Cu}^{\text{II}}(\text{taea})(\text{CH}_3\text{CN})]^{2+}$, $[\text{Cu}^{\text{II}}(\text{tiaea})(\text{CH}_3\text{CN})]^{2+}$ [tren = tris-(2-aminoethyl)amine; taea = tris-(2-ethylaminoethyl)amine; tiaea = tris-(2-isopropylaminoethyl)amine], the reduction was found to proceed through the formation of a thermally unstable $[\text{Cu}^{\text{II}}\text{-NO}]$ intermediate.¹⁸ In cases of $[\text{Cu}(\text{baea})(\text{CH}_3\text{CN})]^{2+}$ [baea = bis-(2-aminoethyl)amine, a tridentate amine donor ligand], and complexes of various bidentate N-donor ligands, such as pymeaa, pyeta, dmeta, deaeta [pymeaa = pyridine-2-methylamine; pieta = pyridine-2-ethylamine; dmeta = *N,N'*-dimethylethylenediamine; deteta = *N,N'*-diethylethylenediamine, *etc.*], the formation of an unstable $[\text{Cu}^{\text{II}}\text{-NO}]$ intermediate was evidenced prior to the reduction of Cu(II) to Cu(I) by nitric oxide.^{19,20} The stability of the $[\text{Cu}^{\text{II}}\text{-NO}]$ intermediate was found to depend on the denticity, chelate ring size and nature of the N-donor atom for these cases. Recently, the example of formation of a stable $[\text{Cu}^{\text{II}}\text{-NO}]$ complex from the reaction of a Cu(II) complex with nitric oxide has been reported.²¹ It would be worth mentioning here that Hayton *et al.* have recently reported the structurally characterized $[\text{Cu}^{\text{II}}\text{-NO}]$ complex, though prepared in a different pathway.²² Interestingly, in cases of Cu(II) complexes having ppmeaa and mimpeaa [ppmeaa, 2-(pyridin-2-yl)-*N*-((pyridin-2-yl)methyl)ethanamine; mimpeaa, *N*-((methyl-1*H*-imidazol-2-yl)methyl)-2-(pyridine-2-yl)ethanamine] ligands, no indication of the formation of an $[\text{Cu}^{\text{II}}\text{-NO}]$ inner-sphere complex has been observed prior to the reduction.²³ This is attributed to the much lower values of the equilibrium constants, K_{NO} (eqn (1)), as reported earlier in the case of $[\text{Cu}(\text{dmp})_2(\text{X})]^{2+}$.¹⁵



The difference in ligand environments, perhaps, leads to a different pathway for the reduction of Cu(II) to Cu(I) by nitric

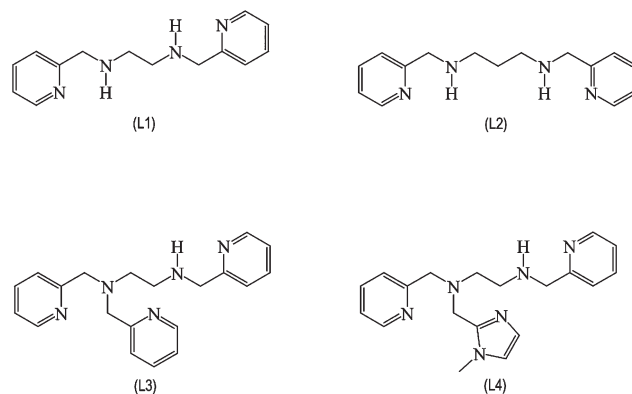


Fig. 1 Ligands used for the present study.

oxide. This has been exemplified by a comparative study of nitric oxide reactivity of $[\text{Cu}(\text{mtad})]^{2+}$ and $[\text{Cu}(\text{tmd})_2]^{2+}$ [mtad = 5,5,7,12,12,14-hexamethyl-1,4,8,11-tetraazacyclotetradecane, tmd = 5,5,7-trimethyl-[1,4]-diazepane].²⁴ It was observed that in the case of $[\text{Cu}(\text{mtad})]^{2+}$, though the reduction takes place through a deprotonation pathway, in $[\text{Cu}(\text{tmd})_2]^{2+}$, it proceeds through a $[\text{Cu}^{\text{II}}\text{-NO}]$ intermediate formation.

In this direction, the nitric oxide reactivities of Cu(II) complexes of the following tetra- and pentadentate ligands (Fig. 1) have been studied to have some insight into the factors which control the reduction mechanism.

Experimental

Materials and methods

All reagents and solvents of reagent grade were purchased from commercial sources and used as received except when specified. Acetonitrile was distilled from calcium hydride. Deoxygenation of the solvent and solutions was effected by repeated vacuum/purge cycles or bubbling with nitrogen for 30 minutes. NO gas was purified by passing through KOH and P_2O_5 columns. UV-visible spectra were recorded on a Perkin Elmer Lambda 25 UV-visible spectrophotometer. FT-IR spectra of the solid samples were taken on a Perkin Elmer spectrophotometer with samples prepared as KBr pellets. Solution electrical conductivity was measured using a Systronic 305 conductivity bridge. $^1\text{H-NMR}$ spectra were recorded in a 400 MHz Varian FT spectrometer. Chemical shifts (ppm) were referenced either with an internal standard (Me_4Si) or to the residual solvent peaks. The X-band Electron Paramagnetic Resonance (EPR) spectra were recorded on a JES-FA200 ESR spectrometer, at room temperature and 77 K with microwave power, 0.998 mW; microwave frequency, 9.14 GHz and modulation amplitude, 2. Elemental analyses were obtained from a Perkin Elmer Series II Analyzer. The magnetic moment of complexes was measured on a Cambridge Magnetic Balance.

Single crystals were grown by slow diffusion followed by a slow evaporation technique. The intensity data were collected

using a Bruker SMART APEX-II CCD diffractometer, equipped with a fine focus 1.75 kW sealed tube MoK α radiation ($\lambda = 0.71073 \text{ \AA}$) at 273(3) K, with increasing ω (width of 0.3° per frame) at a scan speed of 3 s per frame. The SMART software was used for data acquisition. Data integration and reduction were undertaken with SAINT and XPREP software.²⁵ Structures were solved by direct methods using SHELXS-97 and refined with full-matrix least squares on F^2 using SHELXL-97.²⁶ All non-hydrogen atoms were refined anisotropically. Structural illustrations have been drawn with ORTEP-3 for Windows.²⁷ We removed the contribution of smeared electron density from the crystal structure, which we presumed to be due to the disordered water molecules by applying the SQUEEZE of PLATON suite. During squeeze the highest Q peak was changed from 1.14 to 0.64.

Syntheses

Synthesis of L₁. The ligand L₁ was reported earlier.²⁸ To a solution of pyridine-2-carboxaldehyde (2.14 g, 20 mmol) in 20 ml methanol was added ethylenediamine (0.60 g, 10 mmol) into a 50 ml round bottom flask equipped with a stirring bar. The solution was refluxed for 5 h. The resulting reddish-yellow solution was then reduced by NaBH₄ (1.52 g, 40 mmol). Removal of the solvent under reduced pressure affords a crude mass. It was dissolved in water (50 ml) and extracted with chloroform (50 ml \times 4 portions). The organic part was dried under reduced pressure and the reddish yellow oil thus obtained was subjected to chromatographic purification using a silica gel column to yield the pure ligand, L₁ as a yellow oil. Yield: 80%, 1.96 g. Elemental analyses for C₁₄H₁₈N₄: calcd (%): C, 69.39; H, 7.49; N, 23.12. Found (%): C, 69.33; H, 7.50; N, 23.01. FT-IR in KBr: 2791, 1591, 1475, 1431, 767 cm⁻¹. ¹H-NMR (400 MHz, CDCl₃) δ_{ppm} : 2.81 (s, 4H), 3.91 (s, 4H), 7.12–7.15 (t, 2H), 7.30–7.32 (d, 4H), 7.60–7.64 (t, 2H), 8.52–8.53 (d, 2H). ¹³C-NMR (100 MHz, CDCl₃) δ_{ppm} : 46.9, 53.0, 120.7, 121.0, 135.1, 147.6 and 157.6. ESI-Mass ($m + 1$), calcd 243.32; found: 243.04.

Synthesis of L₂. Ligand L₂ was prepared following the same procedure used for L₁ from the reaction of pyridine-2-carboxaldehyde and propylenediamine. Yield, 85%, 2.18 g. Elemental analyses for C₁₅H₂₀N₄: calcd (%): C, 70.28; H, 7.86; N, 21.86. Found (%): C, 70.23; H, 7.85; N, 21.94. FT-IR in KBr: 2791, 1591, 1475, 1430, 1167, 767 cm⁻¹. ¹H-NMR (400 MHz, CDCl₃) δ_{ppm} : 1.75–1.79 (m, 2H), 2.70–2.77 (m, 4H), 3.90 (s, 4H), 7.13–7.16 (t, 4H), 7.28–7.30 (d, 2H), 7.60–7.64 (t, 2H), 7.52–7.54 (d, 2H). ¹³C-NMR (100 MHz, CDCl₃) δ_{ppm} : 29.8, 47.5, 54.8, 121.5, 121.9, 136.0, 148.8 and 159.4. ESI-Mass ($m + 1$): calcd 257.35; found, 257.04.

Synthesis of L₃. L₃ was synthesized by following the reported procedure.²⁹ A solution of 1.21 g (5 mmol) of L₁ and 0.54 g (5 mmol) of pyridine-2-carboxaldehyde in 20 ml of diethyl ether was stirred at room temperature for 3 h to afford a white precipitate. The solid obtained after filtration was washed with diethyl ether. In a 250 ml flask, 1.66 g of the solid

(5 mmol) was dissolved in 50 ml methanol and to this 0.315 g (5 mmol) of NaBH₃CN dissolved in 4 ml methanol and 0.77 ml (10 mmol) of CF₃CO₂H were added. The solution was stirred at room temperature for 8 h. To this NaOH solution (15%, 50 ml) was added and then extracted with CH₂Cl₂ (4 \times 100 ml portions). Removal of the solvent under vacuum affords L₃ as a yellow oil. Yield, 1.26 g, 76%. Elemental analyses for C₂₀H₂₃N₅: calcd (%): C, 72.04; H, 6.95; N, 21.00. Found (%): C, 72.11; H, 6.95; N, 21.10. FT-IR in KBr: 2916, 2786, 1583, 1477, 1432, 765 cm⁻¹. ¹H-NMR (400 MHz, CDCl₃) δ_{ppm} : 2.16 (s, 1H), 2.78 (s, 4H), 3.82 (s, 6H), 7.12–7.15 (m, 4H), 7.27 (d, 1H), 7.51 (d, 1H), 7.59–7.65 (m, 4H), 7.49 (d, 1H). ¹³C-NMR (100 MHz, CDCl₃) δ_{ppm} : 48.8, 54.0, 54.8, 54.9, 60.5, 121.8, 121.8, 121.9, 122.2, 122.2, 123.1, 136.3, 136.4, 148.8, 149.1, 159.4 and 159.6. ESI-Mass ($m + 1$): calcd 334.43; found: 334.78.

Synthesis of the L₄. Ligand L₄ was prepared following the same procedure used for L₃ from the reaction of 1-methylimidazole-2-carboxaldehyde with L₁. Yield 1.21 g, 72%. Elemental analyses for C₁₉H₂₄N₆: calcd (%): C, 67.83; H, 7.19; N, 24.98. Found (%): C, 63.77; H, 7.21; N, 24.89. FT-IR in KBr: 2922, 2803, 1593, 1471, 1432, 1141, 767 cm⁻¹. ¹H-NMR (400 MHz, CDCl₃) δ_{ppm} : 2.71–2.82 (m, 4H), 3.58 (s, 3H), 3.75–3.79 (t, 6H), 6.75 (s, 1H), 6.88 (s, 1H), 7.12–7.16 (m, 2H), 7.25–7.36 (m, 2H), 7.58–7.63 (m, 2H), 8.49–8.53 (m, 2H). ¹³C-NMR (100 MHz, CDCl₃) δ_{ppm} : 32.6, 46.4, 48.8, 53.8, 54.6, 59.9, 121.3, 121.6, 121.8, 121.9, 123.2, 126.7, 136.1, 136.1, 148.7, 148.8, 148.9, 158.8 and 159.5. ESI-Mass ($m + 1$): calcd 337.43; found: 337.22.

Synthesis of complexes

The complexes have been synthesized following a general experimental procedure for the reaction of copper(II) perchlorate, hexahydrate with an equivalent quantity of the respective ligand. The details are given for complex 1.

Complex 1. [Cu^{II}(H₂O)₆](ClO₄)₂ (1.85 g, 5 mmol) was dissolved in 10 ml of distilled acetonitrile. To this solution, L₁ (1.21 g, 5 mmol) was added slowly with constant stirring. The color of the solution turned into greenish-blue from light blue. The stirring was continued for 1 h at room temperature. The volume of the solution was then reduced to \sim 2 ml. To this, benzene (5 ml) was added to layer on it and kept overnight in a freezer. This resulted in dark green color crystalline complex 1. Yield: 2.14 g (85%) and UV-vis. (acetonitrile): λ_{max} , 605 nm ($\epsilon = 245 \text{ M}^{-1} \text{ cm}^{-1}$). X-band EPR (in methanol at 77 K): g_{\parallel} , 2.226; g_{\perp} , 2.012; A_{\parallel} , $160 \times 10^{-4} \text{ cm}^{-1}$. FT-IR (KBr pellet): 3140, 2921, 1608, 1467, 1120, 1083, 625 cm⁻¹. Molar conductivity in acetonitrile, Λ_{M} (S cm⁻¹), 244. μ_{obs} , 1.56 BM.

Complex 2. Complex 2 was synthesized from [Cu^{II}(H₂O)₆](ClO₄)₂ and L₂. Yield: 2.12 g (82%). UV-vis (acetonitrile): λ_{max} , 618 nm ($\epsilon = 166 \text{ M}^{-1} \text{ cm}^{-1}$). X-Band EPR (in methanol at 77 K): g_{\parallel} , 2.270; g_{\perp} , 2.061; A_{\parallel} , $164 \times 10^{-4} \text{ cm}^{-1}$. FT-IR (KBr pellet): 3166, 2866, 1608, 1120, 1082, 765, 625 cm⁻¹. Molar conductivity in acetonitrile, Λ_{M} (S cm⁻¹) 236. μ_{obs} , 1.51 BM.

Complex 3. Complex 3 was synthesized from [Cu^{II}(H₂O)₆](ClO₄)₂ and L₃. Yield: 2.62 g (\sim 88%). UV-vis (acetonitrile): λ_{max} ,

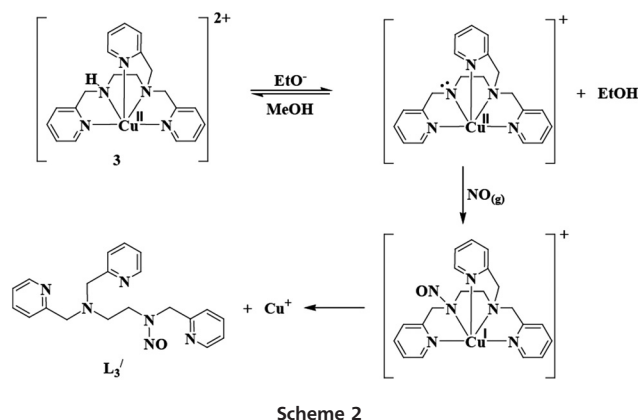
672 nm ($\epsilon = 208 \text{ M}^{-1} \text{ cm}^{-1}$). FT-IR (KBr pellet): 3238, 3077, 1610, 1484, 1144, 1108, 1088, 771, 624 cm^{-1} . X-band EPR (in methanol at 77 K): g_{\parallel} , 2.207; g_{\perp} , 2.013; A_{\parallel} , $158 \times 10^{-4} \text{ cm}^{-1}$. Molar conductivity: Λ_{M} (S cm^{-1}), 205. μ_{obs} , 1.56 BM.

Complex 4. Complex 4 was synthesized from $[\text{Cu}^{\text{II}}(\text{H}_2\text{O})_6](\text{ClO}_4)_2$ and L_4 . Yield: 2.54 g (85%). UV-vis (acetonitrile): λ_{max} , 640 nm ($\epsilon = 173 \text{ M}^{-1} \text{ cm}^{-1}$). The X-band EPR (in methanol at 77 K): g_{\parallel} , 2.230; g_{\perp} , 2.035; A_{\parallel} , $138 \times 10^{-4} \text{ cm}^{-1}$. FT-IR (KBr pellet): 3255, 1611, 1447, 1144, 1108, 1089, 767, 626 cm^{-1} . Molar conductivity in acetonitrile, Λ_{M} (S cm^{-1}), 236. μ_{obs} , 1.54 BM.

Isolation of L_1' . Complex 1 (0.252 g, 0.5 mmol) was dissolved in 10 ml of distilled and degassed methanol. To this solution one equivalent of the sodium ethoxide was added and then the solution was purged with an excess of NO gas. And the resulting colourless solution was stirred for 1 h at room temperature. After removing the excess NO by several cycles of vacuum/purge, 10 ml of degassed benzene was added to this under a dinitrogen atmosphere. The reaction mixture was kept in a freezer overnight. The L_1' -perchlorate was found to be precipitated out. Yield: 133 mg (72%). Elemental analyses for $\text{C}_{14}\text{H}_{22}\text{N}_5\text{ClO}_7$: calcd (%): C, 41.23; H, 5.43; N, 17.17. Found (%): C, 41.15; H, 5.44; N, 17.26. FT-IR (KBr pellet): 3282, 1589, 1437, 1358, 1117, 755, 623 cm^{-1} . $^1\text{H-NMR}$ (400 MHz, D_2O) δ_{ppm} : 4.08–4.13 (2H, t), 4.27–4.34 (2H, t), 4.90 (2H, s), 5.45 (2H, s), 7.22–7.32 (4H, m), 7.69–7.76 (2H, m), 7.57–8.59 (2H, t). $^{13}\text{C-NMR}$ (100 MHz, $\text{D}_2\text{O} + \text{CD}_3\text{CN}$) δ_{ppm} : 43.4, 50.2, 51.8, 58.6, 123.8, 123.9, 123.9, 124.0, 138.4, 138.5, 150.6, 150.9, 155.3, 156.2. ESI-Mass ($m + \text{H}$)/ z : calcd 272.32; found: 272.12.

Isolation of L_2' . L_2' was isolated as its perchlorate salt from the reaction of complex 2 (0.260 g, 0.5 mmol) with nitric oxide following the procedure used for the isolation of the L_1' -perchlorate. Yield: 132 mg (69%). Elemental analyses for $\text{C}_{15}\text{H}_{22}\text{N}_5\text{ClO}_6$: calcd (%): C, 44.62; H, 5.49; N, 17.84. Found (%): C, 42.65; H, 5.49; N, 17.91. FT-IR (KBr pellet): 3067, 2927, 1451, 1437, 1358, 1083, 1123, 755, 629 cm^{-1} . $^1\text{H-NMR}$ (400 MHz, D_2O) δ_{ppm} : 2.36–2.39 (2H, m), 3.60–3.64 (2H, t), 4.32–4.35 (2H, t), 4.87 (2H, s), 5.43 (2H, s), 7.25–7.29 (4H, m), 7.70–7.73 (2H, t), 7.58–8.59 (2H, m). $^{13}\text{C-NMR}$ (100 MHz, $\text{D}_2\text{O} + \text{CD}_3\text{CN}$) δ_{ppm} : 30.2, 42.8, 50.5, 51.9, 58.4, 123.6, 123.8, 123.9, 124.5, 138.1, 138.5, 150.7, 150.9, 155.6, 155.7. ESI-Mass ($m + \text{H}$)/ z : calcd 286.34; found: 286.12.

Isolation of L_3' . L_3' was isolated as L_3' -perchlorate from the reaction of complex 3 (0.305 g, 0.5 mmol) and nitric oxide following the protocol used for L_1' (Scheme 2). Yield: 148 mg (65%). Elemental analyses for $\text{C}_{20}\text{H}_{22}\text{N}_6\text{ClO}_5$: calcd (%): C, 52.01; H, 4.80; N, 18.19. Found (%): C, 52.08; H, 4.81; N, 18.12. FT-IR (KBr pellet): 2936, 1594, 1438, 1118, 1087, 630 cm^{-1} . $^1\text{H-NMR}$ (400 MHz, D_2O) δ_{ppm} : 3.81 (2H, t), 4.46 (2H, t), 4.93 (4H, s), 5.27 (2H, s), 7.14–7.19 (3H, m), 7.36–7.37 (2H), 7.53–7.62 (3H, m), 7.86 (2H), 8.48 (2H). $^{13}\text{C-NMR}$ (100 MHz, $\text{D}_2\text{O} + \text{CD}_3\text{CN}$) δ_{ppm} : 42.8, 49.9, 50.9, 52.7, 61.0, 123.5, 123.8, 123.9, 124.1, 124.3, 124.5, 137.8, 138.1, 135.2, 150.2, 150.6, 150.9, 155.7, 156.7, 160.5. ESI-Mass ($m + \text{H}$)/ z : calcd 363.43; found: 363.45.



Isolation of L_4' . L_4' was isolated from the reaction of complex 4 (0.308 g, 0.5 mmol) with nitric oxide following the procedure used for the isolation of L_3' . Yield: 155 mg (67%). Elemental analyses for $\text{C}_{19}\text{H}_{23}\text{N}_7\text{ClO}_5$: calcd (%): C, 48.67; H, 4.94; N, 20.91. Found (%): C, 48.73; H, 4.94; N, 20.83. FT-IR (KBr pellet): 1598, 1448, 1123, 756, 630 cm^{-1} . $^1\text{H-NMR}$ (400 MHz, D_2O) δ_{ppm} : 2.20 (2H), 3.78 (2H), 4.26 (3H, s), 4.62 (4H, s), 5.02 (2H), 6.61 (1H), 6.80 (1H), 7.14 (2H), 7.65 (2H), 7.83 (2H), 8.46 (2H). $^{13}\text{C-NMR}$ (100 MHz, $\text{D}_2\text{O} + \text{CD}_3\text{CN}$) δ_{ppm} : 33.6, 49.0, 51.3, 51.5, 51.9, 61.0, 123.5, 123.8, 123.9, 124.4, 127.5, 137.8, 136.1, 135.4, 150.1, 150.6, 150.9, 155.6, 160.0. ESI-Mass ($m + \text{H}$)/ z : calcd 366.43; found: 366.37.

Results and discussion

Four Cu(II) complexes, 1, 2, 3 and 4, are synthesized with ligands, L_1 , L_2 , L_3 and L_4 [$\text{L}_1 = \text{N}1, \text{N}2$ -bis((pyridin-2-yl)-methyl) ethane-1,2-diamine, $\text{L}_2 = \text{N}1, \text{N}3$ -bis((pyridin-2-yl)-methyl)-propane-1,3-diamine; $\text{L}_3 = \text{N}1, \text{N}1, \text{N}2$ -tris((pyridin-2-yl)methyl)-ethane-1,2-diamine; $\text{L}_4 = \text{N}1$ -((1-methyl-1H-imidazol-2-yl)methyl)- $\text{N}1, \text{N}2$ -bis((pyridin-2-yl)methyl)ethane-1,2-diamine], respectively, as their perchlorate salts. The complexes are characterized by various analytical techniques (Experimental section). The single crystal structures of all the complexes are determined. The perspective ORTEP views for the complexes 1, 3 and 4 are shown in Fig. 2–4, respectively. Even after several attempts, the crystal quality of complex 2 was not good. The ORTEP view of complex 2 is given in the ESI.† The crystallographic data, important bond distances and angles are listed in Tables 1–3, respectively. In 1 and 2, Cu(II) is found to be surrounded by four nitrogen donor atoms from the respective ligands and two oxygen atoms from two perchlorate ions resulting in an overall distorted octahedral coordination geometry around the Cu center. The Cu–O(perchlorate) distances (2.682/2.592 and 2.697/2.581 Å for 1 and 2, respectively) are within the range of reported Cu–O(perchlorate) distances.^{19,20,23,24} The average Cu–N distances in complexes 1 and 2 are 1.989 Å and 1.994 Å, respectively, which are in the range observed in the reported complexes.^{19,20,23,24}

In complexes 3 and 4, the Cu center is found to be surrounded by five N-atoms from the respective ligands and one

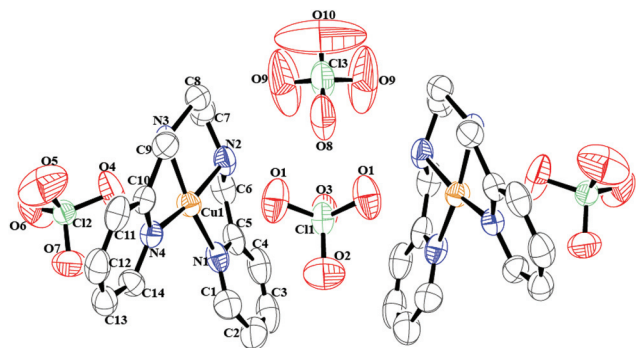


Fig. 2 ORTEP diagram of complex **1** (50% thermal ellipsoid plot; H atoms removed for clarity).

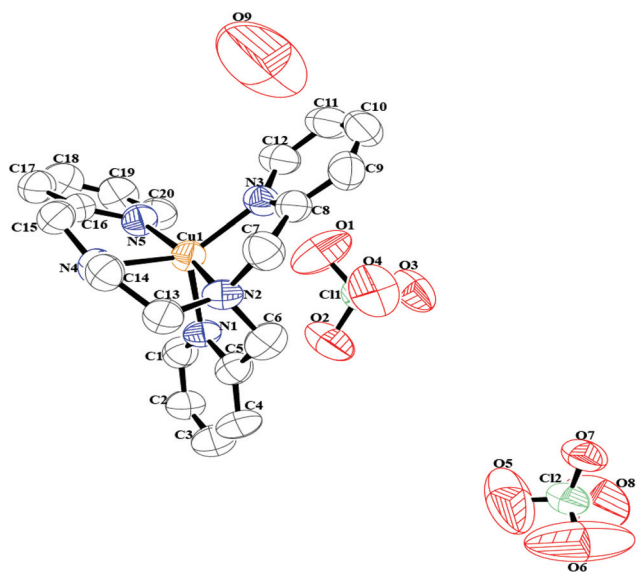


Fig. 3 ORTEP diagram of complex **3** (50% thermal ellipsoid plot; H-atoms removed for clarity).

oxygen atom from a perchlorate anion maintaining an overall distorted octahedral geometry (Fig. 3 and 4). In complex **3**, the four equatorial distances are found to be 1.971, 2.002, 2.026 and 2.041 Å. The axial Cu–N distance (2.102 Å) is observed to be longer compared to the equatorial distances owing to the axial elongation. In complex **4**, the equatorial Cu–N distances are 1.968, 1.987, 2.053 and 2.019 Å and the axial one is 2.137 Å. The Cu–O(perchlorate) distances are 3.967 and 3.900 Å in complexes **3** and **4**, respectively. These distances are a bit longer compared to those observed in complexes **1** and **2** and other reported analogous examples. This suggests a weak interaction between the Cu and the perchlorate anion in these cases.

The complexes **1**, **2**, **3** and **4**, in an acetonitrile solvent, exhibit broad d–d bands at $\lambda_{\max}(\epsilon/M^{-1} \text{ cm}^{-1}) = 605 \text{ nm}$ (245), and 618 nm (170), 672 nm (208), and 640 nm (173), respectively, along with relatively strong intra-ligand absorptions in the UV region (ESI[†]).

The acetonitrile solutions of the complexes displayed characteristic spectra in X-band EPR studies at 77 K (ESI[†]).³⁰ The

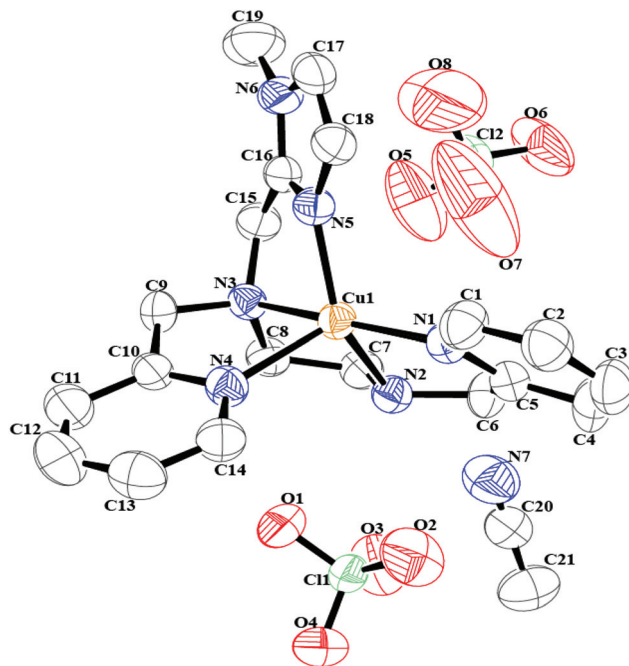


Fig. 4 ORTEP diagram of complex **4** (50% thermal ellipsoid plot; H atoms removed for clarity).

calculated spectral parameters, g_{\parallel} , g_{\perp} and A_{\parallel} , are within the observed range (Experimental section). All the complexes exhibit one electron paramagnetism at room temperature, as expected.

The cyclic voltammetric studies of the pure complexes have been carried out in methanol and acetonitrile solvents. The quasi-reversible couple at -0.55 V versus Ag/Ag^+ in the voltammogram of complex **1** in methanol is attributed to the $\text{Cu}^{\text{II}}/\text{Cu}^{\text{I}}$ process (ESI[†]). This couple appeared at -0.53 and -0.59 V versus Ag/Ag^+ electrode in methanol for complexes **2** and **3**, respectively. However, for complex **4**, an irreversible couple at -0.64 V versus Ag/Ag^+ was appeared (ESI[†]). For $[\text{Cu}(\text{DAC})]^{2+}$, the couple was reported to appear at -0.61 V versus Fc^+/Fc in DMF–MeOH (1 : 1) solution.¹⁶ The differences in potential are attributed to the change in ligand frameworks and denticity. In addition, for complexes **3** and **4**, the change in the axial donor atom from $\text{N}_{(\text{py})}$ to $\text{N}_{(\text{im})}$ may also have an effect on the $\text{Cu}^{\text{II}}/\text{Cu}^{\text{I}}$ potential. For Cu(II) complexes having bidentate N-donor ligands like *N,N*-dimethylethylenediamine, *N,N*-ethylethylenediamine, *N,N*-diisobutylethylenediamine, tmd (tmd = 5,5,7-trimethyl-[1,4]-diazepane), etc., the $\text{Cu}^{\text{II}}/\text{Cu}^{\text{I}}$ couple was also observed to appear in a comparable range.^{20,24} Thus, the ligand denticity and the nature of the donor atoms evidently control the potential for the $\text{Cu}^{\text{II}}/\text{Cu}^{\text{I}}$ couple. The cyclic voltammograms of the complexes in methanol in the presence of one equivalent of sodium ethoxide were also recorded and it shows the expected change in potential due to the formation of the amido anions of the corresponding ligands (ESI[†]).

Nitric oxide reactivity

Nitric oxide reactivities of all the complexes have been studied in dry acetonitrile and methanol solution. However, addition

Table 1 Crystallographic data for complexes **1**, **2**, **3** and **4**

	Complex 1	Complex 2	Complex 3	Complex 4
Formulae	C ₂₈ H ₃₆ Cl ₄ Cu ₂ N ₈ O ₁₆	C ₃₀ H ₃₆ Cl ₃ Cu ₂ N ₈ O ₁₂	C ₂₀ H ₂₂ Cl ₂ CuN ₅ O ₉	C ₂₁ H ₂₇ Cl ₂ CuN ₇ O ₈
Mol. wt.	1009.55	934.12	610.88	639.95
Crystal system	Orthorhombic	Orthorhombic	Monoclinic	Triclinic
Space group	<i>Pnma</i>	<i>Pnma</i>	<i>Pn</i>	<i>P1</i>
Temperature/K	296(2)	296(2)	296(2)	293(2)
Wavelength/Å	0.71073	0.71073	0.71073	0.71073
<i>a</i> /Å	14.4349(13)	13.6904(5)	8.7895(3)	8.9766(2)
<i>b</i> /Å	26.361(3)	26.3804(12)	12.8229(5)	9.9809(2)
<i>c</i> /Å	10.5333(9)	11.3183(5)	11.1763(5)	16.3225(4)
α /°	90.00	90.00	90.00	91.1700(10)
β /°	90.00	90.00	94.308(2)	94.8440(10)
γ /°	90.00	90.00	90.00	110.2890(10)
<i>V</i> /Å ³	4008.1(7)	4089.3(3)	1256.09(9)	1364.84(5)
<i>Z</i>	4	4	2	2
Density/Mg ⁻³	1.673	1.517	1.615	1.557
Abs. coeff./mm ⁻¹	1.406	1.302	1.142	1.054
Abs. correction	Multi-scan	Multi-scan	Multi-scan	Multi-scan
<i>F</i> (000)	2056	1908.0	624	658
Total no. of reflections	4618	5258	5401	6639
Reflections, <i>I</i> > 2σ(<i>I</i>)	3059	2659	3406	3939
Max. 2θ/°	27.67	28.77	28.58	28.43
Ranges (<i>h</i> , <i>k</i> , <i>l</i>)	−18 ≤ <i>h</i> ≤ 17 −30 ≤ <i>k</i> ≤ 34 −13 ≤ <i>l</i> ≤ 13	−18 ≤ <i>h</i> ≤ 16 −35 ≤ <i>k</i> ≤ 26 −14 ≤ <i>l</i> ≤ 15	−11 ≤ <i>h</i> ≤ 11 −17 ≤ <i>k</i> ≤ 14 −15 ≤ <i>l</i> ≤ 14	−12 ≤ <i>h</i> ≤ 11 −13 ≤ <i>k</i> ≤ 12 −21 ≤ <i>l</i> ≤ 21
Complete to 2θ (%)	96.5	96.9	97.5	96.7
Refinement method	Full-matrix least-squares on <i>F</i> ²	Full-matrix least-squares on <i>F</i> ²	Full-matrix least-squares on <i>F</i> ²	Full-matrix least-squares on <i>F</i> ²
Goof (<i>F</i> ²)	1.073	1.016	0.906	0.992
<i>R</i> indices [<i>I</i> > 2σ(<i>I</i>)]	0.0543	0.0943	0.0454	0.0549
<i>R</i> indices (all data)	0.0913	0.1477	0.0719	0.0747

Table 2 Selected bond lengths (Å) for complexes **1**, **2**, **3** and **4**

	Complex 1	Complex 2	Complex 3	Complex 4
Cu(1)–N(1)	1.999(4)	1.990(2)	2.102(4)	1.968(2)
Cu(1)–N(2)	2.003(4)	2.000(3)	2.002(3)	2.019(4)
Cu(1)–N(3)	1.986(4)	2.020(2)	2.026(4)	2.053(2)
Cu(1)–N(4)	1.991(3)	1.990(2)	2.041(4)	2.137(3)
Cu(1)–N(5)	—	—	1.971(4)	1.987(3)
C(1)–C(2)	1.384(8)	1.40(5)	1.371(7)	1.358(5)
C(4)–C(5)	1.374(7)	1.41(5)	1.383(8)	1.384(5)
C(7)–C(8)	1.492(8)	1.42(5)	1.497(9)	1.512(5)
C(10)–C(11)	1.388(6)	1.49(5)	1.39(1)	1.408(6)
C(1)–N(1)	1.327(7)	1.35(4)	1.310(6)	1.349(5)
C(7)–N(2)	1.471(7)	1.29(4)	1.509(7)	1.480(4)
C(8)–N(3)	1.488(6)	—	1.333(8)	1.487(5)

Table 3 Selected bond angles (°) for complexes **1**, **2**, **3** and **4**

	Complex 1	Complex 2	Complex 3	Complex 4
N(1)–Cu(1)–N(2)	82.7(2)	83.0(1)	83.2(1)	83.1(1)
N(1)–Cu(1)–N(3)	167.7(2)	168.0(1)	124.0(2)	166.8(1)
N(1)–Cu(1)–N(4)	110.4(1)	103.8(9)	100.3(2)	108.4(1)
N(1)–Cu(1)–N(5)	—	—	100.3(2)	102.9(1)
N(2)–Cu(1)–N(3)	85.1(2)	93.0(1)	83.5(2)	85.9(1)
N(3)–Cu(1)–N(4)	81.9(2)	82.0(1)	132.3(2)	81.4(1)
N(4)–Cu(1)–N(5)	—	—	83.1(2)	106.7(1)
C(2)–C(1)–N(1)	122.6(5)	122(3)	122.9(5)	122.7(4)
C(1)–C(2)–C(3)	118.3(5)	118(3)	119.6(6)	118.5(4)
C(1)–N(1)–C(5)	118.5(4)	119(2)	118.8(4)	118.7(3)
C(4)–C(5)–C(6)	124.2(4)	123(3)	123.9(5)	122.6(3)

of nitric oxide gas to the acetonitrile solution of the respective complexes was found to be unreactive. In methanol solution, in the presence of one equivalent of sodium ethoxide as a base, the complexes are found to react with nitric oxide leading to the reduction of the Cu(II) center to Cu(I). This has been monitored by UV-visible, X-band EPR spectroscopy. For complex **1**, the d–d band appears with a λ_{\max} at 605 nm in degassed methanol at room temperature. Addition of one equivalent of sodium ethoxide shifted the λ_{\max} to 642 nm (Fig. 5). This is attributed to the formation of the corresponding amido anion coordinated complex after deprotonation at the secondary amine position (Scheme 1).¹⁶ Addition of nitric oxide gas to this solution resulted in immediate decay of the intensity of the absorption band centered at 642 nm and finally disappeared indicating complete reduction of the Cu(II) center to Cu(I) (Fig. 5). It should be noted that similar behaviour was reported for the nitric oxide reactivity of [Cu^{II}(DAC)]²⁺ and [Cu^{II}(mtad)]²⁺ complexes. The spectral changes for the reduction of Cu(II) by nitric oxide in the case of [Cu^{II}(DAC)]²⁺ were observed to be condition dependent. In an unbuffered MeOH–water mixture, the spectroscopic changes appeared to show an induction period which was no longer apparent in the buffered medium. This was, presumably, because of the shift in effective pH in the course of the reaction.¹⁶ In [Cu^{II}(mtad)]²⁺, an induction period was observed in a methanol–water (8 : 2, v/v) medium under unbuffered conditions. The absorbance of a single wavelength (at 523 nm) was plotted *versus* time, however, there was

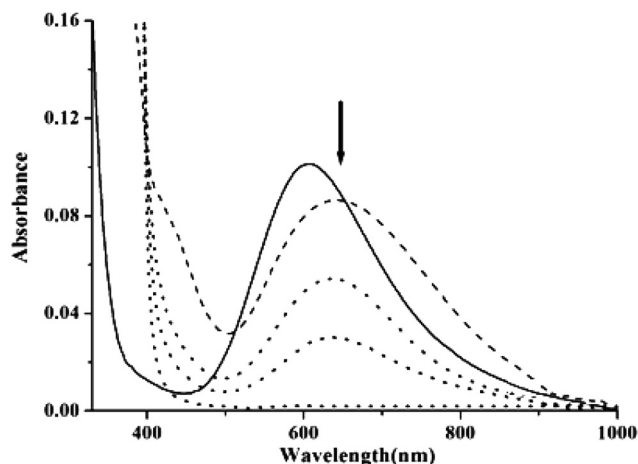


Fig. 5 UV-visible spectra of complex **1** in methanol before (solid line), after (dashed line) addition of one equivalent of sodium ethoxide and after (dotted line) purging nitric oxide.

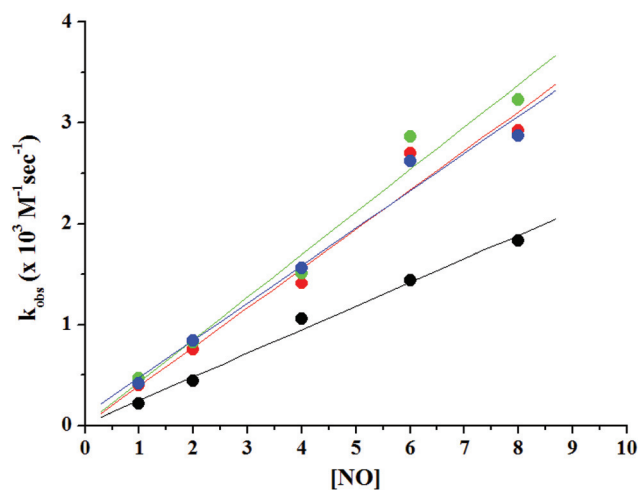


Fig. 6 Plot of k_{obs} vs. equivalent of nitric oxide added to a methanol solution for complexes **1**, **2**, **3** and **4** (black, red, green and blue, respectively) at 298 K.

no indication of the presence of an induction period in a neutral medium.²⁴ In the present study, a shift in λ_{max} from 605 to 642 nm upon addition of one equivalent of sodium ethoxide suggests the formation of the proposed Cu^{II}-amido anion complex, which then reacts with nitric oxide to afford Cu^I from Cu^{II}. This was found to follow a second order rate law which depends on both the [Cu-amido] and [NO]. A plot of rate constants against [NO] at 298 K shows a linear relationship of the rate constants with [NO] at 298 K (Fig. 6).

A similar spectral change was observed in the case of complex **2**, also. The λ_{max} of the d-d band in methanol was shifted from 618 to 664 nm upon addition of one equivalent of sodium ethoxide suggesting the formation of the corresponding Cu^{II}-amido complex (ESI[†]). Addition of nitric oxide gas to this solution was found to diminish the intensity of the d-d band indicating the reduction of the Cu(II) center to Cu(I) following a second order rate equation (Fig. 6).

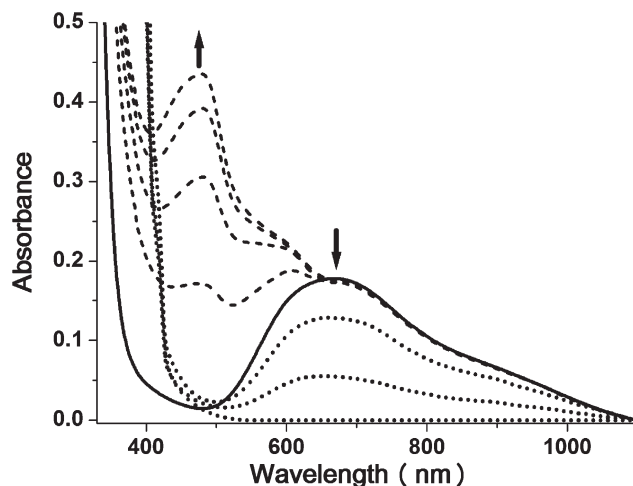


Fig. 7 UV-visible spectra of complex **3** in methanol before (solid line), after (dashed line) addition of one equivalent of sodium ethoxide and after (dotted line) purging nitric oxide.

On the other hand, addition of a base to a methanol solution of complexes **3** and **4** was not found to result in much shifting of λ_{max} like what was observed in cases of complexes **1** and **2**; rather, the appearance of the new absorption bands at ~500 nm in both the cases was observed owing to the formation of the corresponding Cu(II)-amido anion complexes (Fig. 7 and ESI[†]). Upon addition of nitric oxide, these bands were found to diminish gradually along with the corresponding d-d bands owing to the reduction of Cu(II) to Cu(I). The observed rate constants for complexes **3** and **4** are also found to be linearly dependent on [NO] (Fig. 6).

It should be noted that the reduction of the Cu(II) centers was not observed even with four equivalents of NEt₃. On the other hand, as expected, in acidic pH, addition of nitric oxide is not found to reduce the Cu(II) center of the complexes.

In the X-band EPR spectroscopy studies, all the complexes display characteristic signals. Addition of one equivalent of sodium ethoxide to the methanol solution of the complexes resulted in a difference in the *g* values (Fig. 8 and ESI[†]). Nitric oxide purging of these solutions immediately makes them EPR silent. This is because of the formation of diamagnetic Cu(I).

Thus, from the present study it is evident that the reduction mechanism of the Cu(II) center by nitric oxide is very much dependent upon the coordinated ligands framework and denticity. In earlier reports, it was shown that as the macro-cyclic ligands offer extra inertness to the metal center in [Cu(DAC)]²⁺ or [Cu(mtd)]²⁺, the reduction of Cu(II) by nitric oxide does not proceed through the formation of the corresponding [Cu^{II}-NO] intermediate; whereas in cases of analogous non-macro-cyclic ligands, it follows the [Cu^{II}-NO] intermediate pathway. In the present study, though the ligands used are non-macro-cycles, they offer an environment to the metal center which is not susceptible towards the nitric oxide binding to form a [Cu^{II}-NO] intermediate. Now the question arises, which factor plays the most important role in dictating whether the [Cu^{II}-NO]

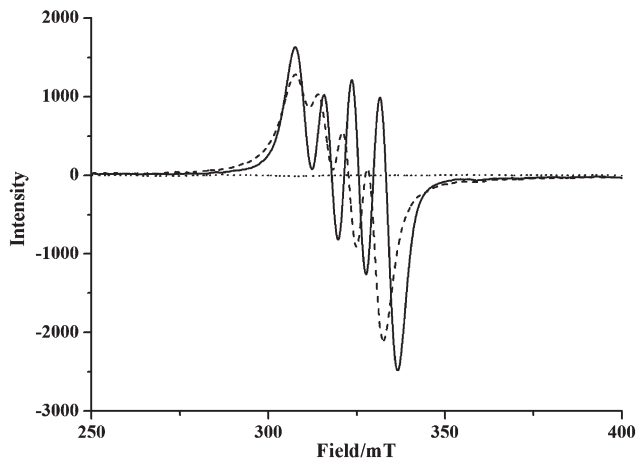


Fig. 8 (a) X-band EPR spectra of complex **1** in methanol before (solid line), after (dashed line) addition of one equivalent of sodium ethoxide and after (dotted line) purging nitric oxide at room temperature.

complex will be formed or not in a particular case? Is it controlled by the donor ability of the ligand (in other words, the electrode potential)? Or, it is a structure dependent phenomenon? In a comparative study of the other reported examples, it has been found that the electrode potential of the $\text{Cu}^{\text{II}}/\text{Cu}^{\text{I}}$ couple essentially does not play much role in the formation of the $[\text{Cu}^{\text{II}}\text{-NO}]$ intermediate. On the other hand, it has been observed that complexes having structural flexibility to attain trigonal-bipyramidal geometry after coordination to the nitric oxide only form the $[\text{Cu}^{\text{II}}\text{-NO}]$ intermediate. For instance, the tetradentate ligands, such as DAC or mtad, because of structural constraints do not allow the corresponding $\text{Cu}(\text{II})$ complex to attain trigonal bipyramidal geometry after nitric oxide coordination. On the other hand, an mtd ligand, which is analogous to mtad, but bidentate offers the required flexibility to the $\text{Cu}(\text{II})$ -nitrosyl complex to attain trigonal bipyramidal geometry very easily. Theoretical studies also suggest a trigonal bipyramidal geometry for this intermediate complex.^{20b,21,24} In cases of all other reported $\text{Cu}(\text{II})$ complexes of bidentate ligands, the formation of the $[\text{Cu}^{\text{II}}\text{-NO}]$ is observed irrespective of the nature of donor atoms. For instance, in pyridine-2-ethyl amine or bemim (bemim = bis-(2-ethyl-4-methylimidazol-5yl)methane), the donor atoms are pyridine and primary amine nitrogen for the former and imidazole nitrogen for the latter; however, the $\text{Cu}(\text{II})$ complexes of these two ligands were found to form a $[\text{Cu}^{\text{II}}\text{-NO}]$ intermediate upon reaction with nitric oxide in acetonitrile solution. The DFT studies again suggested a distorted trigonal bipyramidal geometry for both the cases.^{20b,21,24} In the present study, **L**₁ and **L**₂, being tetradentate and less flexible, do not allow the corresponding $\text{Cu}(\text{II})$ complexes to attain trigonal bipyramidal geometry after nitric oxide coordination. On the other hand, **L**₃ and **L**₄, by virtue, will allow the metal center to form only a hexa-coordinated $[\text{Cu}^{\text{II}}\text{-NO}]$ complex with a distorted octahedral geometry. Thus, the formation of the $\text{Cu}(\text{II})$ -nitrosyl intermediate was not observed in the present study. Hence, it is the structural factor which essentially dictates whether a

particular $\text{Cu}(\text{II})$ complex will form the $\text{Cu}(\text{II})$ -nitrosyl intermediate upon reaction with nitric oxide or not.

The *N*-nitrosated ligands in all the cases have been isolated from the reaction mixture as they were demetallated owing to the weaker donor ability and geometrical preference of $\text{Cu}(\text{I})$ and characterized (Experimental section). In the case of analogous $[\text{Cu}(\text{DAC})]^{2+}$, $[\text{Cu}(\text{mtad})]^{2+}$ complexes, similar results were exemplified.

Conclusion

Thus, the present study demonstrated that the ligand frameworks have a considerable effect in controlling the mechanism of the reduction of a $\text{Cu}(\text{II})$ center by nitric oxide. The flexibility of the ligand/s for a particular $\text{Cu}(\text{II})$ complex to attain a trigonal bipyramidal geometry after NO coordination is found to be the most important parameter in dictating the pathway for their interaction. In the present study, all the four compounds, because of structural constraints, were found to follow a deprotonation pathway for the reduction of a $\text{Cu}(\text{II})$ center by nitric oxide rather than $[\text{Cu}^{\text{II}}\text{-NO}]$ intermediate formation.

Acknowledgements

The authors thank the Department of Science and Technology, India for financial support (SR/S1/IC-38/2010); DST-FIST for X-ray diffraction facility. PK and AK gratefully acknowledge CSIR, India for the fellowship.

References

- (a) *Nitric Oxide: Biology and Pathobiology*, ed. L. J. Ignarro, Academic Press, San Diego, 2000; (b) S. Moncada, R. M. J. Palmer and E. A. Higgs, *Pharmacol. Rev.*, 1991, **43**, 109; (c) A. R. Butler and D. L. Williams, *Chem. Soc. Rev.*, 1993, 233; (d) *Methods in Nitric Oxide Research*, ed. M. Feilisch and J. S. Stamler, John Wiley and Sons, Chichester, England, 1996.
- (a) L. Jia, C. Bonaventura, J. Bonaventura and J. S. Stamler, *Nature*, 1996, **380**, 221; (b) M. T. Galdwin, J. R. Lancaster Jr., B. A. Freeman and A. N. Schechter, *Nat. Med.*, 2003, **9**, 496; (c) R. W. Ye, I. Toro-Suarez, J. M. Tiedje and B. A. Averill, *J. Biol. Chem.*, 1991, **266**, 12848; (d) C. L. Hulse, B. A. Averill and J. M. Tiedje, *J. Am. Chem. Soc.*, 1989, **111**, 2322; (e) M. A. Jackson, J. M. Tiedje and B. A. Averill, *FEBS Lett.*, 1991, **291**, 41.
- (a) J. W. Godden, S. Turley, D. C. Teller, E. T. Adman, M. Y. Liu, W. J. Payne and J. LeGall, *Science*, 1991, **153**, 438; (b) E. T. Adman and S. Turley, in *Bioinorganic Chemistry of Copper*, ed. K. D. Karlin and Z. Tyeklir, Chapman & Hall, Inc., New York, 1993, p. 397; (c) S. J. Ferguson, *Curr. Opin. Chem. Biol.*, 1998, **2**, 182.
- (a) D. J. Richardson and N. J. Watmough, *Curr. Opin. Chem. Biol.*, 1999, **3**, 207; (b) I. Moura and J. J. G. Moura, *Curr.*

- Opin. Chem. Biol.*, 2001, **5**, 168; (c) E. I. Tocheva, F. I. Rosell, A. G. Mauk and M. E. P. Murphy, *Biochemistry*, 2007, **46**, 12366; (d) X. Zhou, M. G. Espey, J. X. Chen, L. J. Hofseth, K. M. Miranda, S. P. Hussain, D. A. Winks and C. C. Harris, *J. Biol. Chem.*, 2000, **275**, 21241.
- 5 (a) J. C. W. Chien, *J. Am. Chem. Soc.*, 1969, **91**, 2166; (b) N. S. Trofimova, A. Y. Safronov and O. Ikeda, *Inorg. Chem.*, 2003, **42**, 1945.
- 6 (a) F. A. Walker, *J. Inorg. Biochem.*, 2005, **99**, 216; (b) D. L. Rousseau, D. Li, M. Couture and S. R. Yeh, *J. Inorg. Biochem.*, 2005, **99**, 306; (c) S. J. George, J. W. A. Allen, S. J. Ferguson and R. N. F. Thorneley, *J. Biol. Chem.*, 2000, **275**, 33231.
- 7 (a) E. Pinakoulaki, S. Gemeinhardt, M. Saraste and C. Varotsis, *J. Biol. Chem.*, 2002, **277**, 23407; (b) V. K. K. Praneeth, F. Paulat, T. C. Berto, S. DeBeer George, C. Nather, C. Sulok and N. Lehnert, *J. Am. Chem. Soc.*, 2008, **130**, 15288; (c) A. V. Soldatova, M. Ibrahim, J. S. Olson, R. S. Czernuszewicz and T. G. Spiro, *J. Am. Chem. Soc.*, 2010, **132**, 4614; (d) I. M. Wasser, S. de Vries, P. Moënne-Loccoz, I. Schröder and K. D. Karlin, *Chem. Rev.*, 2002, **102**, 1201.
- 8 (a) M. Hoshino, M. Maeda, R. Konishi, H. Seki and P. C. Ford, *J. Am. Chem. Soc.*, 1996, **118**, 5702; (b) B. O. Fernandez, I. M. Lorkovic and P. C. Ford, *Inorg. Chem.*, 2004, **43**, 5393; (c) N. Lehnert, V. K. K. Praneeth and F. Paulat, *J. Comput. Chem.*, 2006, **27**, 1338; (d) M. K. Ellison and W. R. Scheidt, *J. Am. Chem. Soc.*, 1999, **121**, 5210; (e) D. P. Linder, K. R. Rodgers, J. Banister, G. R. A. Wyllie, M. K. Ellison and W. R. Scheidt, *J. Am. Chem. Soc.*, 2004, **126**, 14136; (f) M. D. Lim, I. M. Lorkovic and P. C. Ford, *J. Inorg. Biochem.*, 2005, **99**, 151; (g) D. Shamir, I. Zilbermann, E. Maimon, G. Gellerman, H. Cohen and D. Meyerstein, *Eur. J. Inorg. Chem.*, 2007, 5029.
- 9 (a) J. Torres, D. Svistunenko, B. Karlsson, C. E. Cooper and M. T. Wilson, *J. Am. Chem. Soc.*, 2002, **124**, 963; (b) J. Torres, C. E. Cooper and M. T. Wilson, *J. Biol. Chem.*, 1998, **273**, 8756; (c) C. T. Martin, R. H. Morse, R. M. Kanne, H. B. Gray, B. G. Malmstrom and S. I. Chan, *Biochemistry*, 1981, **20**, 5147.
- 10 A. C. F. Gorren, E. de Boer and R. Wever, *Biochim. Biophys. Acta*, 1987, **916**, 38.
- 11 D. Tran and P. C. Ford, *Inorg. Chem.*, 1996, **35**, 2411.
- 12 (a) G. C. Brown, *Biochim. Biophys. Acta*, 2001, **1504**, 46; (b) J. Torres, M. A. Sharpe, A. Rosquist, C. E. Cooper and M. T. Wilson, *FEBS Lett.*, 2000, **475**, 263; (c) H. J. Wijma, G. W. Canters, S. de Vries and M. P. Verbeet, *Biochemistry*, 2004, **43**, 10467.
- 13 B. B. Wayland and L. W. Olson, *J. Am. Chem. Soc.*, 1974, **96**, 6037.
- 14 D. Tran, B. W. Skelton, A. H. White, L. E. Laverman and P. C. Ford, *Inorg. Chem.*, 1998, **37**, 2505.
- 15 M. D. Lim, K. B. Capps, T. B. Karpishin and P. C. Ford, *Nitric Oxide, Biol. Chem.*, 2005, **12**, 244.
- 16 (a) K. Tsuge, F. DeRosa, M. D. Lim and P. C. Ford, *J. Am. Chem. Soc.*, 2004, **126**, 6564; (b) C. Khin, M. D. Lim, K. Tsuge, A. Iretskii, G. Wu and P. C. Ford, *Inorg. Chem.*, 2007, **46**, 9323.
- 17 S. D. Pell and J. N. Armor, *J. Am. Chem. Soc.*, 1973, **95**, 7625.
- 18 (a) M. Sarma, A. Singh, S. G. Gupta, G. Das and B. Mondal, *Inorg. Chim. Acta*, 2010, **363**, 63; (b) M. Sarma, A. Kalita, P. Kumar, A. Singh and B. Mondal, *J. Am. Chem. Soc.*, 2010, **132**, 7846.
- 19 M. Sarma and B. Mondal, *Inorg. Chem.*, 2011, **50**, 3206.
- 20 (a) M. Sarma and B. Mondal, *Dalton Trans.*, 2012, **41**, 2927; (b) M. Sarma, V. Kumar, A. Kalita, R. C. Deka and B. Mondal, *Dalton Trans.*, 2012, **41**, 9543.
- 21 A. Kalita, P. Kumar, R. C. Deka and B. Mondal, *Chem. Commun.*, 2011, **48**, 1551.
- 22 A. M. Wright, G. Wu and T. W. Hayton, *J. Am. Chem. Soc.*, 2010, **132**, 14336.
- 23 P. Kumar, A. Kalita and B. Mondal, *Dalton Trans.*, 2011, **40**, 8656.
- 24 A. Kalita, P. Kumar, R. C. Deka and B. Mondal, *Inorg. Chem.*, 2011, **50**, 11868.
- 25 *SMART, SAINT and XPREP*, Siemens Analytical X-ray Instruments Inc., Madison, Wisconsin, USA, 1995.
- 26 G. M. Sheldrick, *SHELXS-97*, University of Gottingen, Germany, 1997.
- 27 L. J. Farrugia, *J. Appl. Crystallogr.*, 1997, **30**, 565.
- 28 K. Michelsen, *Acta Chem. Scand.*, 1977, **A31**, 429–436.
- 29 P. Mialane, A. Nivorjkin, G. Pratviel, L. Azeéma, M. Slany, F. Godde, A. Simaan, F. Banse, T. Kargar-Grisel, Guy. Bouchoux, J. Sainton, O. Horner, J. Cuilhem, L. Tchertanova, B. Meunier and J. Girerd, *Inorg. Chem.*, 1999, **38**, 1085.
- 30 (a) B. J. Hathaway and A. A. G. Tomlinson, *Coord. Chem. Rev.*, 1970, **5**, 1; (b) B. J. Hathaway, D. E. Billing, P. Nicols and I. M. Procter, *J. Chem. Soc. A*, 1969, 312; (c) B. J. Hathaway, in *Comprehensive Coordination Chemistry*, ed. G. Wilkinson, R. D. Gillard and J. A. McCleverty, Pergamon, Oxford, 1987, vol 5, p. 533; (d) A. K. Patra, M. Ray and R. Mukherjee, *Dalton Trans.*, 1999, 2461.